Electric- and magnetic-field-driven nonlinear charge transport and magnetic ordering in epitaxial films of $Pr_{0.7}Ca_{0.3-x}Sr_xMnO_3$

R. C. Budhani, N. K. Pandey, P. Padhan, and S. Srivastava
Department of Physics, Indian Institute of Technology Kanpur, Kanpur-208016, India

R. P. S. M. Lobo
Laboratoire de Physique des Solides, Ecole Supérieure de Physique et Chimie Industrielles de la Ville de Paris, CNRS UPR 5, 75231 Paris Cedex 5, France

(Received 12 July 2001; published 11 December 2001)

Electric- and magnetic-field-dependent resistivity, and magnetization are studied in epitaxial films of $Pr_{0.7}Ca_{0.3-x}Sr_xMnO_3$ between 4.2 and 300 K. Attention is focused on how the substitution of Sr at the Ca sites of the parent compound $Pr_{0.7}Ca_{0.3}MnO_3$ affects the electrical and magnetic states of this canonical charge-ordered (CO) insulator. The resistivity (ρ) of the parent compound is characterized by a gradual increase on cooling below 300 until 205 K, where it shows a steplike enhancement. We identify this step as the onset temperature (T_{CO}) of the CO state. Below 205 K, a well-defined Arrhenius-type of resistivity with activation energy of 0.13 eV suggests excitation of holes across the CO gap as the mechanism of charge transport in the parent compound. In the films with $x=0.03$ and 0.07, this band-to-band excitation process gives way to a Mott-type, spin-dependent hopping transport from T_{CO} to a crossover temperature T_2 ($<T_{CO}$). Over a narrow temperature range below T_2 and a second crossover temperature T_3, the films show a metallic character followed by the onset of a second insulating state, which persists down to the lowest temperature of measurement (4.2 K). In the regime of temperature between T_2 and 4.2 K, the transport in films with $x=0.03$ and 0.07 is highly nonlinear in electric field, and displays hysteretic and history effects. In this regime of temperature, the resistivity also shows a large drop on application of a magnetic field. In samples with $x\geqslant 0.1$, while the large magnetoresistance in the vicinity of T_2 and the minimum in ρ at T_3 persist, the transport remains Ohmic. Our magnetization measurements show the onset of ferromagnetic ordering in the vicinity of T_2 in all Sr-substituted films. However, for $x<0.1$, a low value of the field-cooled moment and a spin-glass type of behavior seen at temperatures below T_3 suggest formation of ferromagnetic clusters whose moment is gradually blocked with decreasing temperature. We argue that the nonlinear and hysteretic effects seen in samples with $x\leqslant 0.1$ are a result of classical percolation and quantum transport in a topologically inhomogeneous medium.

DOI: 10.1103/PhysRevB.65.014429 PACS number(s): 73.50.Jt

I. INTRODUCTION

The phenomenon of charge ordering (CO) in mixed-valent manganites at certain fractional values of hole concentration has generated much interest in recent years. While a real-space ordering of Mn^{3+} and Mn^{4+} ions in the perovskite $La_{0.5}Ca_{0.5}MnO_3$ was predicted long ago by Goodenough,[1] the parameters controlling the stability of the CO state *vis-à-vis* a charge delocalized ferromagnetic (CDFM) state in these hole-doped compounds have been identified only recently.[2–4] The CO state is insulating and may order antiferromagnetically whereas the CDFM phase is metallic. The sole criterion that decides which of the two states, the CO or CDFM would be more stable at a given temperature is the bandwidth of the lone e_g electron at the Mn^{3+} site. A higher bandwidth facilitated by strong Mn^{3+}-O-Mn^{4+} double exchange interaction favors the CDFM state. If the e_g bandwidth is narrow, as would be the case when the Mn^{3+}-O-Mn^{4+} bond angle deviates significantly from 180°, the contribution to crystal bonding due to the kinetic energy of the delocalized e_g electrons is not significant. The system gains much more energy by undergoing a phase separation where Mn^{3+} and Mn^{4+} ions form two interpenetrating pseudocubic sublattices. Electron transfer between the two sublattices is prohibited, as it would destroy the CO state. Thus, the charge ordering and metallicity in these systems are mutually exclusive. The phenomenological parameter that controls the e_g bandwidth is the average ionic radius $\langle r_A\rangle$ of the rare-earth and the divalent alkaline-earth ions, which occupy the "*A*" site in the $AMnO_3$ manganite unit cell. Generally, for $\langle r_A\rangle\geqslant 1.25$ Å, a CDFM state is more stable, whereas for $\langle r_A\rangle\leqslant 1.22$ Å the system goes to a CO state at lower temperatures. For an intermediate value of $\langle r_A\rangle$, an incipient charge-ordered state is known to form in some half filled systems.[5] The CO state is prone to melting under external perturbation such as strong magnetic fields,[6] electric fields,[7,8] pressure,[9] and high-energy photon flux.[10] The compounds $Pr_{0.7}Ca_{0.3}MnO_3$ and $Pr_{0.5}Ca_{0.5}MnO_3$ are the two extensively studied charge-ordered manganites.[11,12] The average ionic radius in the former is 1.146 Å. It undergoes a robust CO transition in the temperature region 180–250 K followed by an antiferromagnetic transition at ~140 K. At temperatures below 120 K, the system also develops a ferromagnetic component, which has been attributed to the presence of ferromagnetic clusters in the background matrix of the charge-ordered antiferromagnetic (AFM) phase. Since at the dopant concentration (x)

away from some fractional fillings ($\frac{1}{2}$, $\frac{3}{8}$) a long-range ordered CO state is generally not possible, one can argue that these ferromagnetic regions are the natural defects of the CO state. Recent experiments suggest that the CO state in the $Pr_{0.7}Ca_{0.3}MnO_3$ system is weakened if the ''*A*'' site ionic radius is increased by substitution of Pr and/or Ca by the ions of the larger radius. This is manifested by an increase in the magnetic moment and a sharp drop in resistance on cooling below the ferromagnetic transition even in the absence of any perturbation. Substitution of La at Pr and Sr at Ca sites has been tried.[13–17] Raveau, Maignan, and Caignaert[13] have shown that in ceramic samples of $Pr_{0.7}(Ca_{1-x}Sr_x)_{0.3}MnO_3$, an insulator-to-metal transition occurs at $x>0.05$. Lees and co-workers[14] have studied the magnetic phase diagram of $Pr_{0.6}(Ca_{1-x}Sr_x)_{0.4}MnO_3$ ceramic samples. A crossover from the CO to the CDFM state in this case occurs in samples with $x\geqslant 0.25$. A transport and neutron-diffraction study of Yoshizawa *et al.*[9,15] on charge and spin ordering in single-crystal samples of $Pr_{0.65}(Ca_{1-x}Sr_x)_{0.35}MnO_3$ shows that for $x=0.3$ the charge and orbital ordering appear below 200 K as in crystals with $x>0.3$, but collapse into the metallic state below 100 K. Interestingly, these authors see a similar effect when hydrostatic pressure is applied on $Pr_{0.65}Ca_{0.35}MnO_3$ (PCMO) instead of substitution of Sr at the Ca sites. Clearly, the e_g bandwidth seems to play a significant role in deciding the electric and magnetic ground states of the system.

It is important to point out here that a transition to the metallic phase, as detected by resistivity measurements, does not imply a complete conversion of the CO state to the CDFM state. For example, while the resistivity shows an orders-of-magnitude drop, the magnetization does not recover the full value that one would get from counting the Mn^{3+} and Mn^{4+} spins. These observations suggest that the Sr substitution increases the relative abundance of the ferromagnetic clusters seen in the canonical system PCMO, and the metal-insulator transition is a consequence of percolation through these clusters. Measurements of resistivity and magnetization in the $(La_{1-x}Pr_x)_{0.7}Ca_{0.3}MnO_3$ family of manganites[16,17] also suggest a competition for stability between the CO and the CDFM states at low temperatures. The fact that the relative concentrations of the CO and CDFM phases can be varied by applying magnetic field, in addition to changing the La or Sr concentration, make these compounds interesting systems to study percolative transport.

The objective of this paper is to develop an understanding of the topological inhomogenities and the frustrated ground state of the Sr-substituted compounds through measurements of electron transport in the presence of strong electric and magnetic fields. We have carried out these measurements on a series of $Pr_{0.7}Ca_{0.3-x}Sr_xMnO_3$ epitaxial films deposited on single-crystal substrates of $LaAlO_3$ and $SrTiO_3$. Our measurements show that the CO state in $Pr_{0.7}Ca_{0.3}MnO_3$ films is established at $\sim$205 K. The resistivity in this state is thermally activated, indicating a well-defined energy gap of $\sim$0.26 eV. Unlike the case of single crystals, the CO state in films does not show any signs of melting in the electric field (E) and magnetic field (B) as high as 2×10^4 V/cm and 4 T, respectively. The CO state becomes progressively unstable on substitution of Ca by Sr. While the broad features of the magnetoresistance $\rho(B,T)$ and magnetization $M(T)$ of our Sr-substituted films are comparable to those of bulk crystals and ceramic samples, this study of electric-field effects in conjunction with measurements of $\rho(B,T)$ and $M(T)$ reveal many interesting aspects of charge transport in a temperature regime where the system shows magnetic ordering. In samples with $x\geqslant 0.1$, the CO-insulating state gives way to metallic conduction over a range of temperatures whose width is accentuated by the strength of the E and B fields, and by the concentration x. At the lowest temperature, however, the resistivity of these samples again becomes insulatorlike. We have performed detailed measurements of the current-voltage characteristics of the samples with $x<0.1$ in the metallic and the low-temperature insulating regimes. From the hysteretic and history-dependent resistivity seen in these regimes and from the behavior of field-cooled (FC) and zero-field-cooled (ZFC) magnetization, we build a picture of electron transport, which has elements of classical percolation and electric-field-dependent tunneling effects in a topologically inhomogeneous medium.

II. EXPERIMENTAL DETAILS

$Pr_{0.7}Ca_{0.3-x}Sr_xMnO_3$ films were deposited on (001) cut and optically polished substrates of $SrTiO_3$ (STO) and $LaAlO_3$ (LAO) using pulsed laser deposition. A KrF excimer laser (248 nm, Lumonics Model No. 842) beam was focused on a rotating 2-cm diameter target of stoichiometric composition to yield an energy density of $\sim$3 J/cm^2. Highly dense ablation targets were prepared through the standard ceramic route using 99.9% pure $CaCO_3$, $SrCO_3$, Pr_6O_{11}, and Mn_2O_3 as starting materials.[18–20] Film deposition was carried out at 800 °C in 400 mTorr pressure of oxygen. After completion of film deposition, the ablation chamber was back-filled with O_2 to atmospheric pressure, and the sample was cooled to room temperature at the rate of $\sim$5 °C/min. The crystallographic structure of the films was examined in a θ-ω diffractometer using the θ-2θ diffraction mode. The film stoichiometry was checked with Rutherford backscattering (RBS) of 1.6-MeV α particles, and also with electron probe microanalysis on some typical samples. Results of both these measurements were in agreement to within $\pm$2% of the target composition. The RBS technique was also used to ascertain the film thickness, which was in the range of 3500 to 4000 Å for all the compositions reported here. X-ray-diffraction patterns of these films showed an exclusive *c*-axis-oriented growth on the (001) plane of STO and LAO substrates. Since the (001) reflections of the films nearly superimpose the (001) reflections of the substrate, a careful study of the lattice-parameter variation with the Sr concentration could not be carried out.

For electrical measurements, larger area silver pads were evaporated on 2.5×8 mm^2 films through a shadow mask. The silver-coated films were subsequently annealed at 400 °C in flowing oxygen. This is a standard procedure used to lower the contact resistance in oxides such as high-T_c cuprates and manganites. Resistivity measurements were carried out in a liquid-helium cryostat equipped with a 4-T superconducting solenoid. For measurements of I-V curves and the cyclic behavior of resistivity in zero field, we have

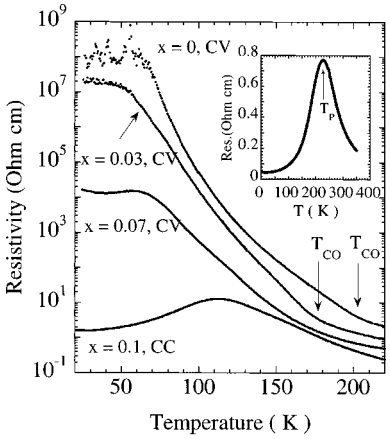

FIG. 1. Electrical resistivity of four $Pr_{0.7}Ca_{0.3-x}Sr_xMnO_3$ films with Sr concentrations $x=0$, 0.03, 0.07, and 0.1, plotted as a function of temperature over the range 20–220 K. Notations CV and CC denote constant voltage and constant current, respectively. Arrows in the figure indicate the onset of charge ordering. The zero-field resistivity of a film of the end member $Pr_{0.7}Sr_{0.3}MnO_3$ is shown in the inset.

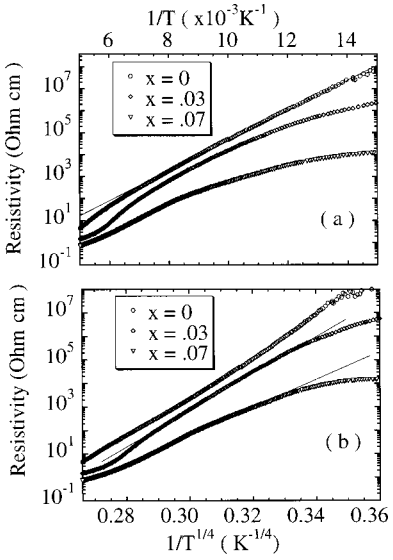

FIG. 2. Arrhenius plots of the resistivity of the films with $x=0.0$, 0.03, and 0.07 are shown in (a). The solid line in the figure is the Arrhenius fit to the resistivity of the Sr-free film. The same data are plotted as a function of $(1/T)^{1/4}$ in (b), and the solid line are fits to the variable-range-hopping formula.

used a closed-cycle helium refrigerator, which goes down to ~20 K. Both two-probe and four-probe methods have been used for resistivity measurements in the constant-voltage as well as constant-current modes. In the first case, a fixed or variable voltage was applied across the sample, and the current flow was monitored by measuring the voltage drop across a metal film resistor. The constant-current mode measurements of magnetoresistance were carried out using a precision dc current source and a nanovoltmeter. The magnetization data was obtained in a Quantum Design superconducting quantum interference device magnetometer.

III. RESULTS

We first present the results of resistivity measurements in zero magnetic field over the temperature range 20–300 K (Fig. 1). The standard four-probe method of resistance measurements could not be used in Sr-deficient films due to their high resistance and the limited input impedance (10 GΩ) of our voltmeter. We have measured the resistivity of the samples with $x=0.0$, 0.03, and 0.07 using the constant-voltage method. In order to avoid heating of the samples at higher temperatures where their resistance is quite small, an order-of-magnitude smaller voltage was used in these measurements. For the sample with $x=0.1$, the data were taken in the constant-current mode. In all the samples, the resistivity first increases on cooling below room temperature. A distinct shoulder in the resistivity of the samples with $x=0$ and 0.03, as marked by arrows in the figure, corresponds to the onset of the charge-ordered state (T_{CO}). Below T_{CO}, the resistivity of the sample with $x=0$ increases rapidly and becomes higher than what could be measured with our setup. But as x increases, the resistivity at the lowest temperature drops. Its temperature dependence is also strikingly different. In the Sr-substituted samples, the resistivity on cooling first reaches a peak value followed by a local minimum and finally an increase at the lowest temperatures. This peak is much more prominent in samples with $x=0.1$. For the sake of comparison, in the inset of Fig. 1 we show the ρ vs T data for a film with $x=0.3$. The bell-shaped resistivity curve with a peak at ~230 K seen here is typical of a double exchange ferromagnetic manganite.

In the bulk samples of the end member $Pr_{0.7}Sr_{0.3}MnO_3$, the peak in resistivity corresponds to the onset of the ferromagnetic state. The temperature of the peak T_p in ceramic samples is ~240 K.[11] In the case of films, however, the T_p is highly sensitive to the deposition conditions and the degree of lattice match between the film and the substrate. A T_p of as low as ~130 K has been reported in $Pr_{0.7}Sr_{0.3}MnO_3$ films deposited on a $SrTiO_3$ substrate.[21] A high T_p in our case suggests that these films are relatively stress-free and have an oxygen stoichiometry close to the bulk value. The rapid rise of resistivity on decreasing the temperature until $T\sim T_p$ indicates the dominance of thermally activated transport. In a sample where the charge ordering is robust and a clear signature of T_{CO} is seen in the ρ vs T data, one would expect the transport below T_{CO} to be due to carrier excitation across the charge-ordering gap. The resistivity of the Sr-free sample indeed shows an Arrhenius type of thermally activated conduction below T_{CO} [Fig. 2(a)]. The energy gap determined from this measurement is ~0.26 eV. Spectroscopic measurements of the CO gap in manganites yield a value of the same order of magnitude.[22,23] However, significant deviations from the Arrhenius type of behavior are seen with increasing x. In fact, for the films with $x=0.03$ and 0.07, the resistivity below T_{CO} is in much better agreement with the Mott variable-range-hopping (VRH) formula.[24] The VRH transport leads to a resistivity of the type $\rho(T)=\rho_0\exp[(T_0/T)^{1/4}]$, where ρ_0 is a preexponential factor and T_0 is related to the density of states at the Fermi level $N(E_F)$ through the relation k_BT_0

$=18\alpha^3/N(E_F)$. The solid lines in the figure are fits to this phonon-assisted-tunneling process. From these fits one can calculate the localization length ($a=1/\alpha$). The values of k_BT_0 for the samples with $x=0.03$ and 0.07 are 84 439 and 31 397 eV, respectively. The density of states at E_F calculated from the coefficient of the linear term (γ) in the specific heat of the compound $Pr_{0.6}(Ca_{0.75}Sr_{0.25})_{0.4}MnO_3$, which is 4.72 $mJ\,mol^{-1}K^{-2}$,[14] comes out to be $\sim 3.5 \times 10^{28}\,eV^{-1}m^{-3}$. This leads to a localization length of 0.026 nm for the sample with $x=0.07$. This is a rather unphysical value considering the fact that the localization length should be at least of the order of the Mn-O bond length. Two factors can lead to a gross discrepancy in the estimation of "a" from the specific-heat data in these systems. It has been shown by Smolyaninova *et al.*[25] that a γ term as large as 30 $mJ\,mol^{-1}K^{-2}$ can exist in the charge-ordered insulator $Pr_{0.7}Ca_{0.3}MnO_3$ in which one does not expect any density of states at the E_F. The source of a large γ here is the spin and charge disorder and resulting two-level states seen in classic spin-glass systems. Clearly, these contributions to γ would result in an overestimation of $N(E_F)$ and a much smaller localization length.

In this analysis of thermally activated conduction, we have also not taken into consideration the relative orientation of the manganese $3d$ spins at the site from which the electron leaves and the site to which it goes. A parallel orientation of spins at these sites strongly favors the hopping process. Consideration of this effect renormalizes the density of state at the Fermi energy.[26] Application of a magnetic field promotes parallel spin orientation at the hopping sites, and thus, the effective density of states for tunneling.

A. Electric-field effects

In a single crystal of the charge-ordered manganite $Pr_{0.7}Ca_{0.3}MnO_3$, Asamitzu, Tomioka, and Tokura[7] observed a highly electric-field-dependent conductivity above a threshold field of $\sim 10^3$ V/cm at temperatures below the Néel temperature ($T_N \sim 170$ K). These authors attributed this effect to electric-field-induced melting of the CO state and the ensuing metallic conduction. We have measured the electrical resistivity of the pure and Sr-substituted PCMO films as a function of temperature at several values of electric field. Unlike the case of single crystals, which show a conductivity jump in the AFM state at $E \geqslant 10^3$ V/cm, the $Pr_{0.7}Ca_{0.3}MnO_3$ film remains highly insulating below $T \sim 80$ K at fields as high as 2×10^4 V/cm. We believe that unlike the case of crystals, the persistence of the high-resistivity state in these films is due to a substrate-induced strain, which may pin the CO state. Some thick films of this compound, when annealed at $T > 900\,^\circ$C did switch to a low-resistivity state at high voltages. But the behavior was sample dependent.

The resistivity of the sample with 0.03 Sr per formula unit is, however, highly sensitive to electric field in the region of temperature below 85 K. In Fig. 3, we show the resistivity of a $Pr_{0.7}Ca_{0.27}Sr_{0.03}MnO_3$ film on (100) $SrTiO_3$ measured in the constant-voltage mode as a function of increasing temperature. Two distinct regimes of behavior can be identified in the data taken at the lowest electric field. Between 25 K and T_2,

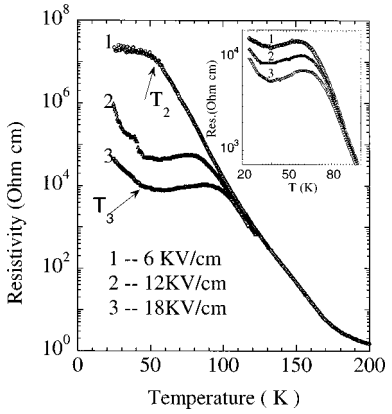

FIG. 3. Electrical resistivity of a $Pr_{0.7}Ca_{0.27}Sr_{0.03}MnO_3$ film measured in the constant-voltage mode at three values of electric field. The onset temperature of charge ordering (T_{CO}) and the crossover temperatures T_2 and T_3 are marked by arrows in the figure. Inset shows the resistivity of the film with $x=0.07$ at three values of electric field.

the resistivity shows a slow drop with temperature, followed by a marked thermally activated conduction between T_2 and T_{CO}. When the electric field is increased by a factor of 2, a considerably lower value of ρ is seen at 25 K. The resistivity drops with temperature until a minimum is reached at T_3, and then a metal-like behavior follows over a small range of temperatures. Measurements at the next-higher field show that the metal-like regime is wider and the resistance at T_3 is considerably lower. At temperatures above ~ 100 K, the behavior of ρ at all fields is similar. This pronounced effect of electric field on the resistivity of these manganite thin films diminishes as the Sr concentration is increased. To illustrate this point, in the inset of Fig. 3 we show the resistivity of the film with Sr$=0.07$. Here the drop in resistance at T_3 on increasing the field to 18 kV/cm is only by a factor of 2.3 as compared to the three orders-of-magnitude drop seen in the case of the film with $x=0.03$. For the sample with $x=0.1$, the resistivity remains perfectly Ohmic throughout the temperature range between 25 K and room temperature. The electric-field-dependent resistivity of the samples with $x=0.03$ and 0.07 is, however, not a monotonic function of E. In Fig. 4, we show a series of I-V curves for the sample with $x=0.03$ taken at several temperatures. For each of these measurements, the sample was first cooled in zero electric field to the desired temperature and then the field was scanned at a constant rate from zero to a maximum value followed by a reverse scan to zero field. As evident in the figure, the sample shows a remarkable switching to a low resistance state when a critical value of the electric field is reached. This is highlighted by the logarithmic scale used for the Y axis in the figure. On field reversal, however, the behavior is hysteretic with current following Ohm's law. Subsequent field scans at the same temperature and also at higher temperatures do not reveal the hysteresis. The behavior remains Ohmic in both directions of the field scan. The high-resistivity state, the off state, is however recovered if the sample is warmed to a temperature above T_{CO}. The I-V curves of the sample with $x=0.03$ show three characteristic

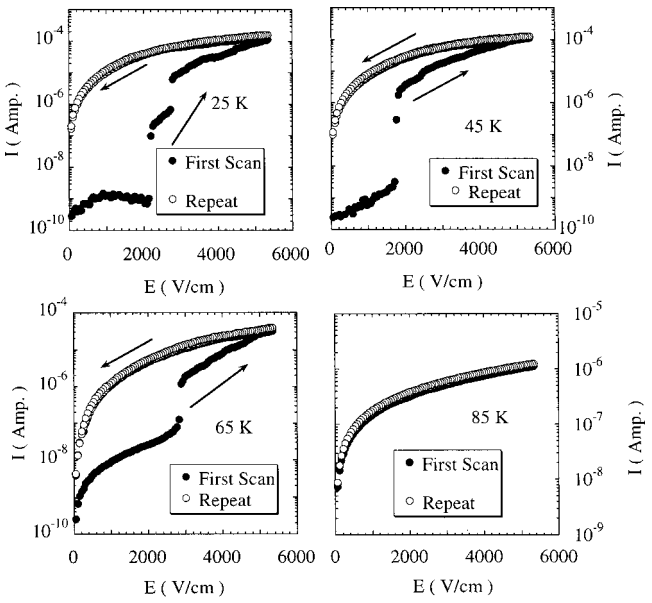

FIG. 4. Current-electric-field (I-E) characteristics of the $Pr_{0.7}Ca_{0.27}Sr_{0.03}MnO_3$ film at 25, 45, 65, and 85 K. Both first and repeat scans taken at a given temperature are shown (see text for details).

features on increasing the temperatures: (i) the switching field to the low-resistivity state decreases, (ii) the area under the hysteresis shrinks, and (iii) at temperatures above 85 K the behavior is fully reversible. An additional feature of the data shown in Fig. 4 is the steplike increase in current at certain values of the electric field. In semiconductor physics, such steps are associated with emptying of the midgap traps by the electric field. In the present case, however, the value of the electric field at which the steps occur is sample and history dependent.

The I-V curves of the sample with $x=0.07$ are quite different. While the current in this case also shows a nonlinear increase with the electric field and the behavior is hysteretic on field reversal, there are no steps in the response. However, as for the sample with $x=0.03$, the I-V curves at $T=85$ K and above do not show any hysteresis. The history effects in this sample are also similar. An interesting aspect of the current transport in these samples is revealed when we plot the resistivity as a function of the reciprocal of the electric field ($1/E$). The data for the sample with $x=0.07$ are shown in Fig. 5 for the field-increasing branch of the hysteresis. The crisscrossing of the ρ vs $1/E$ curves taken at different temperatures seen in the figure is actually due to the minimum at $T\sim 40$ K in the resistivity vs temperature curves measured at different field strengths (see inset, Fig. 3). At 65 and 75 K, the resistivity is Ohmic at $E\leqslant 10^3$ V/cm whereas at lower temperatures a clear field-activated behavior is seen over a large range of electric field. This type of electrical conduction has been observed in a variety of materials. For example, in granular films consisting of metallic particles in a dielectric host, the low-temperature resistivity below the percolation threshold varies with field as $\rho=\rho_0\exp[E_0/E]$, where ρ_0 is the preexponential factor and E_0 is related to the dielectric constant of the insulating matrix and the topology

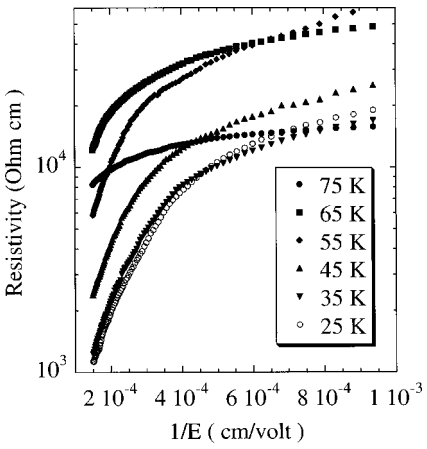

FIG. 5. Resistivity of the $Pr_{0.7}Ca_{0.23}Sr_{0.07}MnO_3$ film at different temperatures plotted as a function of $1/E$. The data emphasize the $\exp(E_0/E)$ dependence of the resistivity at high electric fields.

of the metallic channels.[27,28] The value of E_0 in our case is $\sim 8\times 10^3$ V/cm, and it is temperature independent. This behavior is characteristically similar to that of Ni-SiO_2 inhomogeneous films.[27–29] At higher temperatures, when k_BT becomes comparable to the potential difference between the neighboring grains, thermally activated tunneling dominates over the field-induced process. In this region the conductivity is Ohmic.

B. Electron transport in the presence of a longitudinal magnetic field

We have measured the resistivity of our samples over the temperature range 4.2–350 K while a dc magnetic field of strength $\leqslant 4$ T was applied parallel to the direction of current through the sample. There is a curious identity between the effects of electric and magnetic fields on the electron transport. This is seen in Fig. 6 where we plot ρ vs T for the

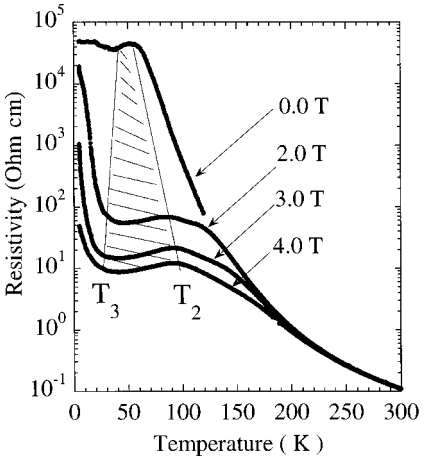

FIG. 6. Temperature dependence of the resistivity of the $Pr_{0.7}Ca_{0.23}Sr_{0.07}MnO_3$ film measured in the presence of a magnetic field. The direction of the field was parallel to the direction of current through the sample. The shaded area between temperatures T_2 and T_3 in the figure emphasizes the regime of temperature and field over which the sample is metallic.

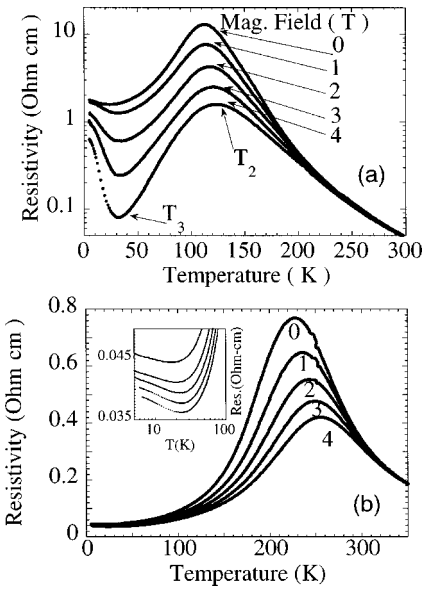

FIG. 7. (a) The resistivity of the $Pr_{0.7}Ca_{0.2}Sr_{0.1}MnO_3$ film measured as a function of temperature at several values of magnetic field. Panel (b) shows results of similar measurements on the end member ($Pr_{0.7}Sr_{0.3}MnO_3$). Inset of (b) shows the $\ln(1/T)$ divergence of the resistivity at the lowest temperature.

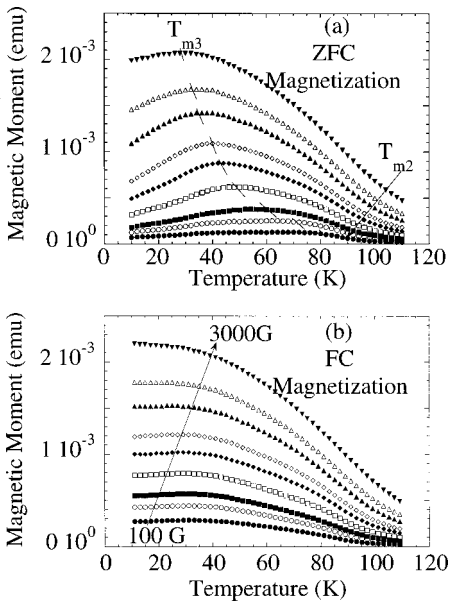

FIG. 8. (a) Zero-field-cooled and (b) field-cooled magnetization of a $Pr_{0.7}Ca_{0.27}Sr_{0.03}MnO_3$ film plotted as a function of temperature. The magnetic fields used in these measurements are 100, 200, 300, 500, 750, 1000, 1500, 2000, and 3000 G from the bottom curve to the top curve. The crossover temperatures T_{m2} and T_{m3} are shown in panel (a).

sample with $x=0.07$ at several values of the magnetic field. These are constant-current measurements in which the electric field was kept below ~200 V/cm. Further, the maximum resistance measured in these experiments is 1% of the input impedance (10 GΩ) of the voltmeter. In order to highlight the drastic effects of a magnetic field on the resistivity, Fig. 6 also shows the zero-field data for the same sample. This measurement, however, had to be done in the constant-voltage mode ($E\sim 4$ kV/cm) because of the impedance-related limitations of the constant-current method. In zero magnetic field, the resistivity of the sample is thermally activated for $T>55$ K. However, at 2 T this behavior is truncated below ~130 K and the resistivity shows a plateau down to ~35 K followed by a rapid increase at still lower temperatures. At higher fields, we see a further drop in resistance and the behavior in the range ~35–100 K is metallike. However, below ~35 K a marginally insulating behavior persists even at 4 T. Using the convention of Fig. 3, we define the temperature at which metallic conduction sets in on cooling as T_2 and the temperature of the minimum as T_3. In the shaded region, between the contours of these two temperatures, the system is metallic. A similar behavior is seen in the resistivity of the sample with $x=0.03$, albeit with a much narrower metallic region.

On increasing x further to 0.1, the zero-field resistivity at 4.2 K drops by four orders of magnitude as compared to the resistivity of the sample with $x=0.07$. As seen in Fig. 7(a), the ρ vs T curves of this sample at several fields mimic the behavior of a typical double exchange ferromagnetic manganite such as $La_{0.7}Ca_{0.3}MnO_3$ (LCMO) but for the minimum seen at T_3. The pronounced peak in resistivity occurring at ~110 K at zero field shifts to higher temperatures and its height decreases on increasing field strength. This trend is identical to the behavior of the resistivity in LCMO near the Curie temperature. The minimum at T_3 seen here appears to be a terminal manifestation of the process, which leads to the marked insulating behavior below T_3 in samples with $x=0.03$ and 0.07. However, unlike the samples with the lesser amount of Sr, the response of the system in this case remains Ohmic at $T<T_3$. Interestingly, even the films of the end member ($Pr_{0.7}Sr_{0.3}MnO_3$) show a slight upturn in resistivity at very low temperatures [Fig. 7(b)]. It appears that the observed minimum is a compound effect of the closing percolation channels and localization by impurity disorder in a narrow band. The former process may be relevant in the Ca-rich and the latter in the Sr-rich compounds. We will discuss this issue further in the subsequent section.

C. Magnetization measurements

Since the charge transport in manganites is intimately linked with their magnetic state, for any discussion on electron transport it is imperative to have a knowledge of the magnetic correlations in these materials. We have carried out zero-field-cooled (ZFC) and field-cooled (FC) magnetization measurements on our samples at several values of the applied magnetic field. In Fig. 8(a) we show the ZFC magnetization as a function of temperature of a film with $x=0.07$. The FC magnetization of the same film is shown in Fig. 8(b). At the lowest field (100 G), the ZFC magnetization first increases rapidly and then slowly with temperature until a peak value is reached at ~80 K. Between 80 and 100 K, the ZFC magnetization shows a rapid drop, and above 100 K, the magnetization is very small. We identify these temperatures as T_{m3} and T_{m2}, respectively. The FC magnetiza-

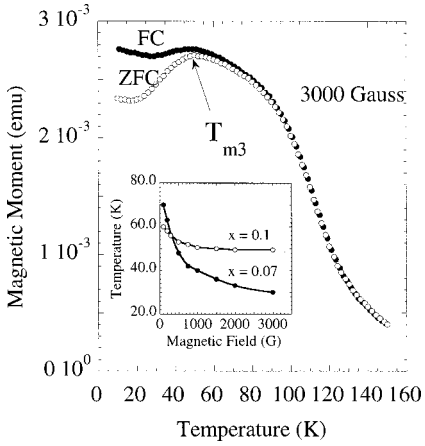

FIG. 9. FC and ZFC magnetization of a $Pr_{0.7}Ca_{0.2}Sr_{0.1}MnO_3$ film measured as a function of temperature at a 3000-G field. Inset shows the variation of the crossover temperature T_{3m} (as defined in the text) with field for two samples with $x=0.07$ and 0.1.

tion shows a similar rise at T_{m2} but the FC and ZFC values do not coincide below a well-defined temperature. The FC moment remains high until the lowest temperature of measurement. This spin-glass type of behavior seen here can arise from ferromagnetic clusters whose moments are gradually blocked with decreasing temperature. We tentatively call it a glassy phase of giant spin molecules. The general features of the FC and ZFC magnetization in films with $x=0$ and 0.03 are similar. While it is difficult to calculate the absolute moment per Mn site for samples in a thin-film geometry, qualitatively, there is a systematic increase in the value of the FC magnetization at $T=10\,\mathrm{K}$ with x, and the irreversible magnetization $M_{\mathrm{irr}}(10\,\mathrm{K})=M_{\mathrm{FC}}(10\,\mathrm{K})-M_{\mathrm{ZFC}}(10\,\mathrm{K})$ decreases with increasing x. In films with $x=0.1$, the moment at the lowest temperature is considerably higher as seen in typical ZFC and FC curves taken at 3000-G field (Fig. 9). However, the drop in the ZFC moment at $T<T_{m3}$ is still present in this case. In the inset of Fig. 9 we plot the variation of T_{m3} for the samples with $x=0.07$ and 0.1. In the sample with $x=0.15$, while T_{m2} is pushed to much higher temperatures, there is no evidence of a crossover temperature T_{m3} below which the ZFC magnetization drops. Clearly, the glassy behavior in magnetization is confined to $x<0.1$.

IV. DISCUSSION

The electron transport in the canonical charge-ordered manganite PCMO is controlled by excitations across the charge-order gap and the short- and long-range ferromagnetic correlations. Neutron-scattering studies[11,12,30] on this system clearly indicate the onset of a ferromagnetic moment at $T\sim 120\,\mathrm{K}$ in the charge-ordered antiferromagnetic background. While this ferromagnetic component can be ascribed either to nucleation of a ferromagnetic clusters phase in the AFM background or to a noncollinear magnetic structure, local probes[30–32] seem to suggest that the former is perhaps a better description for the ferromagnetic component. The insulator-to-metal transition driven by irradiation with x rays,[33] electrons,[34] and short pulses of photons[10] further suggests nucleation, growth, and coalescence of such clusters/islands under these perturbations. Optical reflectivity measurements also show how metal-like channels develop in $Pr_{0.7}Ca_{0.3}MnO_3$ on simultaneous application of dc electric and photon fields.[35] In the following section we apply the concept of preexisting ferromagnetic clusters/islands, which are metallic, to discuss electron transport in our films. From our magnetization measurements we infer that the relative abundance of such clusters increases with x, and at sufficiently high values of x (>0.15), a fully ferromagnetic state develops. However, here it is important to point out that the substrate-induced stresses in thin-film samples may change, to some degree, the Sr concentration above which the CDFM state is stable. Millis, Darling, and Migliori[36] have argued that the lattice strain affects the CDFM state in two ways. While a uniform compression may reduce the electron-lattice coupling, a biaxial strain will increase the tendency for localization. The strain effects are pronounced in ultrathin films of manganites deposited on substrates where the lattice mismatch is large, such as LAO.[37] The lattice strain is, however, released as the film thickness becomes larger. We expect the effects of strain to be minimal in these relatively thick films.

Electron transport, superconductivity, and magnetism in inhomogeneous media consisting of metal particles in a dielectric host lattice have been discussed within the framework of classical percolation models, and also quantum mechanically taking into account electron tunneling, localization, and quantization of electronic levels in the microscopic particle/clusters.[27,38,39] The different energies that control electronic motion from cluster to cluster and lead to the flow of a macroscopic current through a microscopically inhomogeneous sample are the following: (i) The magnetic coupling energy. If the bulk magnetization vectors of the two neighboring clusters i and j are $\mathbf{M}_i$ and $\mathbf{M}_j$, respectively, the energy barrier for electron transfer between them can be written as $U(\theta_{ij})=U_0(1-\cos\theta_{ij})$, where θ_{ij} is the angle between the two moments. This barrier is maximum when the moments are antiparallel. (ii) Electrostatic charging energy. The metallic clusters embedded in an insulating host have a capacitance, which depends on the size and shape of the clusters, and also, on the effective dielectric constant of the medium. If an extra electron or hole is to be placed on a cluster, it is necessary to provide the energy of the electrostatic field associated with the extra charge carrier. The charging energy E_c is $\sim e^2/(Kd)$, where K is the dielectric constant of the medium, and d the diameter of the cluster. (iii) Quantization effects. Finally, for a microscopic metallic particle one must consider the discreteness in the otherwise continuum of states near E_F because of the particle-in-a-box-like situation. The spacing between the metal-like state is given as[27]

$$\delta=8E_F/\pi d^3 n, \tag{1}$$

where E_F is the Fermi energy and n the number of conduction electrons per unit volume of the metallic phase. In addition, one more energy scale that enters the picture is the

width of each of these states due to a finite lifetime τ_L of a hole/electron in a given cluster before it tunnels into a neighboring cluster.

If we neglect the magnetic part of the interaction for a moment, then the problem can be mapped onto the problem of electron transport in granular films of nonmagnetic metals. Two regimes of behavior can be identified in such films.[27] (i) A low-voltage–high-temperature regime, such that the biasing energy ($e\Delta V$) across the clusters is much smaller than the charging energy E_c, and $K_BT \geqslant \delta$. This leads to a thermally activated resistivity of the form

$$\rho = \rho_0 \exp[2\sqrt{(C/K_BT)}] \tag{2}$$

where C and ρ_0 are constants. (ii) A high-voltage–low-temperature regime, in which case a carrier is injected over the Coulomb gap that opens up in the tunneling density of states due to charging. However, if $K_BT \ll \delta$, and $e\Delta V \ll \delta$, an injected hole may not find an energy level of matching energy in the neighboring cluster. The charge transfer is then possible only via emission or absorption of a phonon. Optimization of these three processes and their dependence on the cluster size make the conductivity a scale-dependent quantity.

At low temperatures when $e\Delta V \ll \delta$, the field-dependent resistivity can be written as

$$\rho = \rho_\infty \exp[E_0/E], \tag{3}$$

where ρ_∞ is a temperature-dependent preexponent, E the applied electric field, and E_0 a constant related to the electrostatic barrier.

The above model of electron transport needs to be extended in order to be applicable to magnetically inhomogeneous charge-ordered manganites. The following points need to be considered: (i) in zero magnetic field, tunneling will take place only between those grains whose moments are nearly parallel. (ii) The external magnetic field will align the random moments and an increase in the tunneling sites will result. The external magnetic field may also increase the number and size of ferromagnetic clusters. (iii) The role of electric field is also to increase the number of tunneling sites. This fact is already incorporated in Eq. (3), and the sharp drop in resistance with increasing fields as seen in Fig. 5 is consistent with this picture. However, while this scenario successfully explains the initial drop in resistance, a metallike conduction as seen between temperatures T_2 and T_3 (Fig. 3) will not result unless the metallic clusters coalesce and open a conducting channel across the sample. The existence of such channels is seen in the reflectivity data of PCMO.[35] A logical picture for conduction, albeit needing some mathematical rigor to strengthen it, is the following. The thinnest sections of the CO-insulating matrix between closely spaced metallic clusters are melted by the forced transport of holes between the clusters. The melted links are ferromagnetic and metallic. The metallic channel presumably remains open when the electric field is brought back to zero, and this results in Ohmic resistivity as seen in the reverse branch of the I-V curves (Fig. 4). In order to reestablish the CO state, the sample needs to be warmed to a temperature above T_{CO}. This process of opening the metallic ferromagnetic channels has elements of self-organization and criticality as evident from the steps in the I-V curves.

The disappearance of metallic transport at $T > T_2$ is linked intimately with the disappearance of ferromagnetic order. Magnetization measurements on these samples show a T_c of 80 K at $x=0$. The T_c increases with x. The resistivity data of Figs. 3 and 6 strongly suggest that above T_c, the charge ordering is reestablished in the clusters and the resistivity smoothly joins the ρ vs T curves taken in the absence of a magnetic field and at lower values of the electric field.

The temperature dependence of electrical conduction in samples with $x=0.1$ and 1.0 [Figs. 7(a) and 7(b)] is characterized by thermally activated conduction on cooling below 350 K until a temperature where long-range ferromagnetic order develops in the system. A switchover in conduction to a metallic behavior results in a peak in the resistivity. In the regime of temperatures near the peak, we see a large negative magnetoresistance. These features are typical of a ferromagnetic manganite although the absolute value of resistivity is much larger for the sample with $x=0.1$. The behavior of resistivity in the paramagnetic state has been discussed at length in recent years.[40–42] In one picture, the self-trapped e_g electron forms a magnetically dressed lattice polaron, which conducts via hopping. The insulating behavior may also result due to localization of the e_g electron in a random spin-dependent potential. Both of these formalisms lead to a resistivity that follows the Mott variable range hopping for a three-dimensional disordered system. Coey *et al.*[42] have argued that the spin-polarized nature of the e_g electrons makes them susceptible to trapping in ferromagnetic regions when the overall magnetic order deviates from perfect collinearity. This results in a steep increase in resistivity on approaching T_c. Such ferromagnetically ordered regions have been christened as giant spin molecules. The behavior of resistivity in the ferromagnetic metallic and paramagnetic insulating phases agrees quantitatively with this model.

The issue of much more interest here is the minimum in the resistivity seen in Figs. 6, 7(a), and the inset of 7(b). While this feature is generally observed in epitaxial films of some metallic manganites,[43] its origin has hardly been discussed. A similar feature is also seen in marginally doped lanthanum vanadates,[44] hole-doped La_2CuO_4,[45] and the magnetic pyrochlores.[46] In the following section we discuss this issue and raise some questions with the hope that it will generate further interest in understanding the resistivity minima. One explanation that is plausible at least for the compounds with $x=0.1$ is based on the concept of magnetic granularing, which we used to explain the minimum in the sample with $x<0.1$. One could argue that in the sample with $x=0.1$ there is still some vestige of the insulating phase between the ferromagnetic clusters. The tunneling density of states will have a gap of the order of the charging energy of the clusters. Since the cluster size is now quite large, E_c is insignificant compared to K_BT at the higher temperatures. This would result in metallic conduction at higher temperatures. But at sufficiently low temperatures, holes must be transferred between the clusters by the phonon-assisted-tunneling processes. As the phonon population density goes

down, the resistivity increases. However, the idea of having an insulating shell all around the ferromagnetic grains does not apply in the case of the end member $Pr_{0.7}Sr_{0.3}MnO_3$, which does not charge order. A scenario where holes hop between the giant spin molecules would also not lead to a low-temperature insulating behavior because the barrier for hopping, $\sim U_H(1-\cos\phi)$, decreases with temperature. An acceptable explanation perhaps lies in the random potential fluctuations due to Pr^{3+} and Sr^{2+} ion cores experienced by the e_g electrons, which may lead to weak localization.[47] The resistivity below the minimum indeed shows a $\ln(1/T)$ divergence characteristic of weak localization. A rigorous treatment of this effect, however, requires measurement of resistivity to still lower temperatures and estimation of Coulomb interactions between the carriers,[48] which also lead to an upturn in the resistivity at low temperatures.

V. SUMMARY

The primary objective of this paper was to study the nonlinear electrical transport and the electric-field-driven insulator-to-metal transition in $Pr_{0.7}Ca_{0.3-x}Sr_xMnO_3$ manganites, where the relative concentrations of Ca and Sr control the bandwidth of the e_g electrons. Our studies have been performed on epitaxial thin-film samples because of the inherent ease a film geometry offers in studies of high electric-field effects at moderately low applied voltages. Our *in situ* grown epitaxial films of the parent compound PCMO switch from a paramagnetic insulating state to a charge-ordered insulating state on cooling through ~205 K. In the CO state, the resistivity of these films is thermally activated. A uniquely defined activation energy for transport over a broad temperature range below ~205 K suggests the opening of a gap in the CO state. As in the case of ceramic and bulk single-crystal samples, these films also show the onset of a weak ferromagnetic ordering at $T\sim 80$ K. However, unlike the case of the crystals where the Co state melts on application of an electric field $\sim 1\times 10^3$ V/cm the CO state in the films remains robust in electric field as high as 2×10^4 V/cm.

The charge transport becomes progressively susceptible to electric and magnetic fields on substitution of Ca by Sr. In samples with $x<0.1$, the CO state becomes metallic over a temperature range whose width is accentuated by the strengths of the E and B fields, and by the concentration x. At the lowest temperature, however, the resistivity of these samples again becomes insulatorlike. We observe a correlation between the upper (T_2) and lower (T_3) temperatures, which bound the metallic regime, and the temperatures T_{2m} and T_{3m}, which characterize the onset and blocking temperatures of the ferromagnetic moment, respectively. Measurements of current-voltage characteristics in this temperature regime reveal a highly nonlinear, hysteretic and history-dependent transport. Fascinating current switching effects, in which the resistance drops by ~six orders of magnitude, are also seen in this regime in samples with 0.03 Sr. Samples with $x\geqslant 0.1$ show Ohmic transport over the entire temperature range. These samples are metallic below the Curie temperature, albeit for a logarithmic divergence of the resistivity at the lowest temperature. From the measurements of I-V curves, resistivity, and FC and ZFC magnetization, we infer that the samples with $x<0.1$ are microscopically inhomogeneous, consisting of ferromagnetic metallic clusters in a charge-ordered insulating matrix. The transport in such inhomogeneous systems has elements of classical percolation and electric-field-induced tunneling.

ACKNOWLEDGMENTS

This work has been supported by a grant from the Department of Science and Technology, Government of India. We wish to thank Dr. V. N. Kulkarni and R. K. Rakshit for help in RBS measurements. Part of this paper was written while R.C.B. was on sabbatical at the Center for Superconductivity Research, University of Maryland. He thanks Professor R. L. Greene and Professor C. J. Lobb for their hospitality. He also acknowledges stimulating discussions with R. L. Greene, C. J. Lobb, Vera Smolyaninova, and Amlan Biswas. R.P.S.M.L. thanks CNRS-ESPCI for financial support. The discussions with P. Monod are greatly appreciated.

[1] J. B. Goodenough, Phys. Rev. **100**, 564 (1955).
[2] C. N. R. Rao and A. K. Raychaudhuri, in *Colossal Magnetoresistance, Charge Ordering and Related Properties of Manganese Oxides*, edited by C. N. R. Rao and B. Raveau (World Scientific, Singapore, 1998), p. 1.
[3] M. Imada, A. Fujimori, and Y. Tokura, Rev. Mod. Phys. **70**, 1039 (1998).
[4] E. Dagotto, T. Hotta, and A. Moreo, Phys. Rep. **344**, 1 (2001).
[5] A. Arulraj, A. Biswas, A. K. Raychaudhuri, C. N. R. Rao, P. M. Woodward, T. Vogt, D. E. Cox, and A. K. Cheetham, Phys. Rev. B **57**, R8115 (1998).
[6] H. Kuwahara, Y. Tomioka, A. Asamitsu, Y. Moritomo, and Y. Tokura, Science **270**, 961 (1995).
[7] A. Asamitsu, Y. Tomioka, and Y. Tokura, Nature (London) **388**, 50 (1997).
[8] C. N. R. Rao, A. R. Raju, V. Ponnambalam, S. Parasar, and N. Kumar, Phys. Rev. B **61**, 594 (2000).
[9] H. Yoshizawa, R. Kajimoto, H. Kawano, Y. Tomioka, and Y. Tokura, Phys. Rev. B **55**, 2729 (1997).
[10] K. Miyano, T. Tanaka, Y. Tomioka, and Y. Tokura, Phys. Rev. Lett. **78**, 4257 (1997).
[11] Z. Jirak, S. Krupicka, Z. Simsa, M. Dlouha, and Z. Vratislav, J. Magn. Magn. Mater. **53**, 153 (1985).
[12] D. E. Cox, P. G. Radaelli, M. Marezio, and S.-W. Cheong, Phys. Rev. B **57**, 3305 (1998).
[13] B. Raveau, A. Maignan, and V. Caignaert, J. Solid State Chem. **117**, 424 (1995).
[14] M. R. Lees, O. A. Petrenko, G. Balakrishnan, and D. McK Paul, Phys. Rev. B **59**, 1298 (1999).
[15] Y. Tomioka, A. Asamitsu, H. Kuwahara, and Y. Tokura, J. Phys. Soc. Jpn. **66**, 302 (1997).

[16] K. H. Kim, M. Uehara, C. Hess, P. A. Sharma, and S.-W. Cheong, Phys. Rev. Lett. **84**, 2961 (2000).
[17] N. A. Babushkina, L. M. Belova, D. I. Khomskii, K. I. Kugel, O. Yu. Gorbenko, and A. R. Kaul, Phys. Rev. B **59**, 6994 (1999).
[18] C. Roy and R. C. Budhani, J. Appl. Phys. **85**, 3124 (1999).
[19] R. C. Budhani, C. Roy, L. H. Lewis, Q. Li, and A. R. Moodenbaugh, J. Appl. Phys. **87**, 2490 (2000).
[20] S. Srivastava, N. K. Pandey, P. Padhan, and R. C. Budhani, Phys. Rev. B **62**, 13 868 (2000).
[21] M. Rajeswari, A. Goyal, A. K. Raychaudhuri, M. C. Robson, G. C. Xiong, C. Kwon, R. Ramesh, R. L. Greene, T. Venkatesan, and S. Lakeou, Appl. Phys. Lett. **69**, 851 (1996).
[22] A. Biswas, A. K. Raychaudhuri, R. Mahendiran, A. Guha, R. Mahesh, and C. N. R. Rao, J. Phys.: Condens. Matter **9**, L355 (1997).
[23] A. Chaainani, H. Kumigashira, T. Takahashi, Y. Tomioka, H. Kuwahara, and Y. Tokura, Phys. Rev. B **56**, R15 513 (1997).
[24] N. F. Mott and E. A. Davies, *Electronic Processes in Non-Crystalline Solids*, 2nd ed. (Oxford University Press, New York, 1979).
[25] V. N. Smolyaninova, A. Biswas, X. Zhang, K. H. Kim, B. G. Kim, S.-W. Cheong, and R. L. Greene, Phys. Rev. B **62**, R6093 (2000).
[26] M. Viret, L. Ranno, and J. M. D. Coey, Phys. Rev. B **55**, 8067 (1997).
[27] B. Abeles, P. Sheng, M. D. Coutts, and Y. Arie, Adv. Phys. **24**, 407 (1975).
[28] J. I. Gittleman, Y. Goldstein, and S. Bozowski, Phys. Rev. B **5**, 3609 (1972).
[29] F. Millange, S. de Brion, and G. Chouteau, Phys. Rev. B **62**, 5619 (2000).
[30] J. W. Lynn, R. W. Erwin, J. A. Borchers, Q. Huang, A. Santoro, J. L. Peng, and Z. Y. Li, Phys. Rev. Lett. **76**, 4046 (1996).
[31] M. Uehara, S. Mori, C. H. Chen, and S. W. Cheong, Nature (London) **399**, 560 (1999).
[32] J. M. De Teresa, M. R. Ibarra, P. A. Algarabel, C. Ritter, C. Marquina, J. Blasco, J. Garcia, A. Del Moral, and Z. Arnold, Nature (London) **386**, 256 (1997).
[33] V. Kiryukhin, D. Casa, J. P. Hill, B. Keimer, A. Vigliante, Y. Tomioka, and Y. Tokura, Nature (London) **385**, 813 (1997).
[34] M. Hervieu, A. Barnabe, C. Martin, A. Maignan, and B. Raveau, Phys. Rev. B **60**, R726 (1999).
[35] M. Feibig, K. Mayano, Y. Tomioka, and Y. Tokura, Science **280**, 1925 (1998).
[36] A. J. Millis, T. Darling, and A. Migliori, J. Appl. Phys. **83**, 1588 (1998).
[37] P. Padhan, N. K. Pandey, S. Srivastava, R. K. Rakshit, V. N. Kulkarni, and R. C. Budhani, Solid State Commun. **117**, 27 (2001).
[38] Y. Imry and M. Strongin, Phys. Rev. B **24**, 6353 (1981).
[39] S. Kirkpatrick, Rev. Mod. Phys. **45**, 574 (1972).
[40] A. Millis, B. I. Shraiman, and P. B. Littlewood, Phys. Rev. Lett. **74**, 514 (1995).
[41] M. Jaime, M. B. Salamon, M. Rubinstein, R. E. Treece, J. S. Horwitz, and D. B. Chrisey, Phys. Rev. B **54**, 11 914 (1996).
[42] J. M. D. Coey, M. Viret, L. Ranno, and K. Ounadjela, Phys. Rev. Lett. **75**, 3910 (1975).
[43] Y. Sawaki, K. Takenaka, A. Osuka, R. Shiozaki, and S. Sugai, Phys. Rev. B **61**, 11 588 (2000).
[44] F. Inaba, T. Arima, T. Ishibawa, T. Katsufuji, and Y. Tokura, Phys. Rev. B **52**, R2221 (1995).
[45] H. Takagi, B. Batlogg, H. L. Kao, J. Kwo, R. J. Cava, J. J. Krajewski, and W. F. Peck, Phys. Rev. Lett. **69**, 2975 (1992).
[46] Y. Moritomo, A. Asamitzu, H. Kuwahara, and Y. Tokura, Nature (London) **380**, 141 (1996).
[47] P. A. Lee and T. V. Ramakrishnan, Rev. Mod. Phys. **57**, 287 (1985).
[48] B. L. Altshuler and A. G. Aronov, in *Electron-Electron Interactions in Disordered Systems*, edited by M. Pollak and A. L. Efros (North-Holland, Amsterdam, 1985), p. 1.